

# Effects of Bragg Mirror Interface Grading and Layer Thickness Variations on VCSEL Performance at 1.55 $\mu\text{m}$

M. Linnik and A. Christou

Department of Materials and Nuclear Engineering and Center for OptoElectronic Devices, Packaging and Interconnects (COEDIP), University of Maryland, College Park, MD 20742

## ABSTRACT

A selectively oxidized Vertical Cavity Surface Emitting Laser (VCSEL) has been designed and fabricated for operation at a wavelength of 1.546 $\mu\text{m}$ . The lattice matched device structure was grown on an InP substrate using III-V quaternary semiconductor alloys for Bragg mirrors and GaInAsP-based unstrained Multi-Quantum Wells (MQW) for the active layer. The mirror reflectivities are 97% for the top Distributed Bragg Reflector (DBR) consisting of 16 pairs of AlGaInAs/InP layers, and 99.9% for the bottom DBR consisting of 22 pairs. A threshold current as low as 2.2mA has been achieved. The threshold voltage was typically lower than 2.0 V and the power output exceeded 1mW. The laser spectrum from a 7 $\mu\text{m}$  confined diode shows a single mode of operation at 1.54  $\mu\text{m}$ . The single fundamental mode was present at all current levels. The influence of the intentional and growth-related compositional grading at the heterointerfaces as well as random and fixed thickness variations of layer thickness on the mirror reflectivity and laser characteristics has been investigated, and key sensitivities to laser performance have been determined through computational simulations. It is shown that the degree of surface roughness and random thickness variation have the strongest impact on the device performance.

**Keywords:** VCSEL, DBR, composition grading, random thickness variation, reflectivity, threshold current.

## 1. INTRODUCTION

Compound semiconductor based long wavelength surface emitting lasers are becoming important light sources for large capacity optical communications and optical interconnection systems. Those devices exhibit such advantages as low threshold currents, single mode operation, high coupling efficiencies into optical fiber<sup>1</sup>, and high speed modulation<sup>2</sup>. Quarter-wave Distributed Bragg Reflectors (DBRs) of high reflectivity are extensively used in the optical devices such as VCSELs. Low threshold current operation of the surface emitting laser depends heavily on the performance of Bragg mirrors.

High quality Bragg mirrors for VCSEL applications are characterized by high reflectivity and low series resistance of the stack. The large index of refraction difference between the alternating layers in Bragg mirrors is responsible for high optical reflectivity, at the same time the large band gap difference at the hetero-interfaces results in impediment of the carrier flow leading to large series resistance of the stack. High series resistance gives rise to the thermal heating and deterioration of the laser performance. It was reported by Fastenau *et al*<sup>3</sup> that by using graded interfaces the DBR series resistance can be reduced by two orders of magnitude compared to abrupt interfaces. Other approaches to reduce series resistance of the DBR include heavy doping, parabolic grading and modulation doping to create a flat valence band at the interface<sup>4</sup>.

Because it is difficult to have a perfect control over growth thickness and alloy composition of the mirror layers, the effect of variations in these parameters on the reflectivity spectrum and other laser characteristics has to be taken into account. The thickness variations investigated include random variations around a nominal thickness, a fixed bias in thickness added during growth, effect of surface roughness, and interdiffusion at the hetero-interfaces during growth. Such variations were found to be a common occurrence during epitaxial mirror growth.

In this paper, we report a low threshold all epitaxial VCSEL structure which is based on III-V quaternary semiconductor alloys and is grown by MBE. Theoretical studies of the effect of various intentional and growth-related composition grading at the heterointerfaces on the DBR reflectivity and VCSEL threshold current are presented, in addition to laser performance results. We also present the result of absorption measurements for a sample having a 5% interface grading as well as 20% grading. The quaternary semiconductor alloys were selected in order to achieve the highest reflectivity of Bragg mirror with the smallest number of periods.

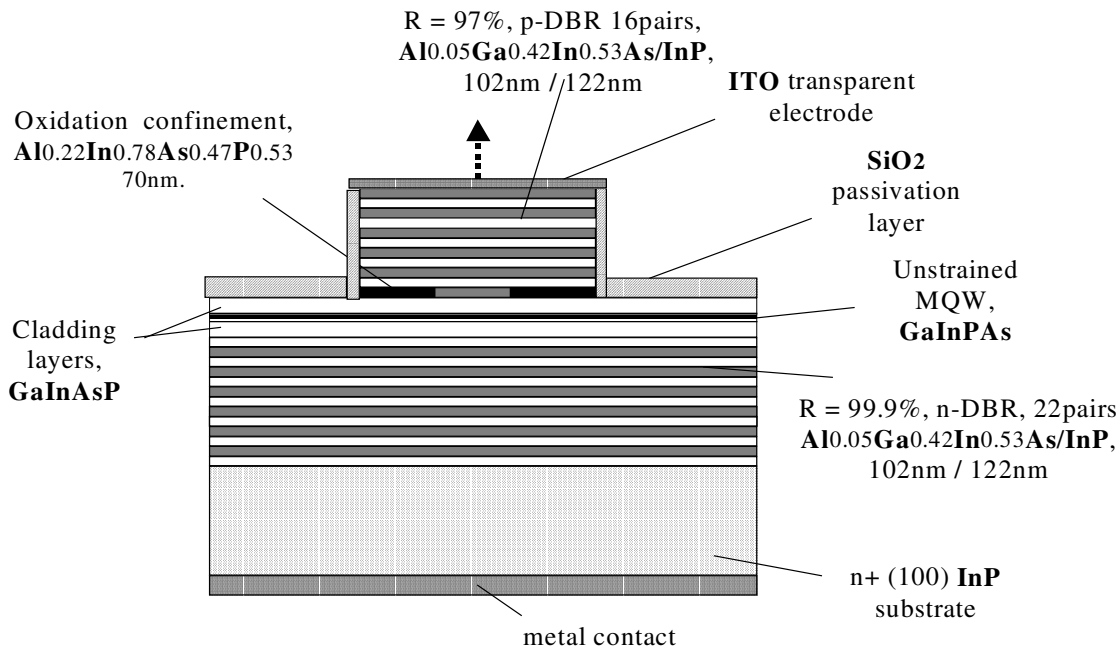
## 2. VCSEL STRUCTURE DESIGN

Quaternary III-V semi-conductor alloys offer a high degree of flexibility in variation of their electro-optical properties. In order to predict the dielectric constant behavior of the quaternary alloy, we initially consider the energy band gap dependence on the composition of quaternary semiconductor alloys. These results are then used for the calculation of the dielectric constant, which in turn allows us to select the alloys leading to the largest index of refraction contrast ratio.

The estimation of the composition dependence of the quaternary semiconductor alloy energy gap has been demonstrated by Moon *et al.*<sup>5</sup>, and is based on the material parameters of the four corresponding binary constituents. These parameters include values of the direct and indirect energy band gaps of the binary compounds as well as the bowing parameters of the ternary compounds.

The method used for the calculation of the real and imaginary parts of the dielectric constant has been reported by Adachi<sup>6</sup>. It is based on a simplified model of the band structure of the materials<sup>7</sup> and covers the optical response of the semiconductors over the entire range of the photon energies. By calculating the imaginary part of the dielectric constant,  $\epsilon_2$ , using the Kramers-Kronig relationships, and assuming parabolic behavior of the energy band gap of the semiconductor, the real part of the dielectric constant,  $\epsilon_1$ , is obtained. As a result of this investigation, two material systems have been selected that are lattice matched to InP substrate and demonstrate the largest contrast between their refractive indices.  $\text{Al}_{0.05}\text{Ga}_{0.42}\text{In}_{0.53}\text{As}$  and InP alloys have refractive indices of 3.8 and 3.17, respectively, resulting in refractive index difference of 0.63.

The investigated VCSEL schematically presented in Figure 1, is fabricated on n-type (001) InP substrate and includes two DBRs, cladding layers, unstrained MQW active layer and oxidizing layer where all materials are lattice matched to the substrate.



**Figure 1.** Schematic representation of the designed VCSEL structure.

The MQW structure in the present work grown by molecular beam epitaxy is unstrained and not intentionally doped. The MQW active region lasing at 1.546 $\mu\text{m}$  was theoretically designed and optimized, consisting of eight  $\text{Ga}_{0.43}\text{In}_{0.57}\text{As}_{0.92}\text{P}_{0.08}$  wells, 6nm thick, separated by seven  $\text{Ga}_{0.23}\text{In}_{0.77}\text{As}_{0.5}\text{P}_{0.5}$  barriers, 9nm thick. The band gaps of the well ( $E_g = 0.78\text{eV}$ ) and barrier ( $E_g = 1.0\text{eV}$ ) layers were optimized to obtain the largest conduction band discontinuity for a sufficient quantum size effect of electrons<sup>8</sup>. The MQW layer was located at the peak of the electric field standing wave in order to achieve matched gain. The active region is spaced by the cladding layers:  $\text{Ga}_{0.11}\text{In}_{0.89}\text{As}_{0.24}\text{P}_{0.76}$  and  $\text{Ga}_{0.03}\text{In}_{0.97}\text{As}_{0.07}\text{P}_{0.93}$ , with energy band gaps 1.2eV and 1.31eV, respectively. The thickness of  $\text{Ga}_{0.11}\text{In}_{0.89}\text{As}_{0.24}\text{P}_{0.76}$  top cladding layer is 20nm, and  $\text{Ga}_{0.03}\text{In}_{0.97}\text{As}_{0.07}\text{P}_{0.93}$  second top cladding layer is 81.6nm thick.  $\text{Ga}_{0.11}\text{In}_{0.89}\text{As}_{0.24}\text{P}_{0.76}$  bottom cladding layer is 70nm thick and  $\text{Ga}_{0.03}\text{In}_{0.97}\text{As}_{0.07}\text{P}_{0.93}$  bottom cladding layer is 101.6nm thick.

A single  $\text{Al}_{0.22}\text{In}_{0.78}\text{As}_{0.47}\text{P}_{0.53}$  layer, 70nm thick, is introduced as the lowest layer in the p-type DBR next to the cladding layers to be used for selective oxidation in order to improve VCSEL efficiency through selective oxidation formation of an aperture<sup>9</sup>. The insulating buried oxide efficiently confines the charge carriers into the laser active region while the reduced refractive index of the oxide transversely confines the laser emission. In addition, the larger Al mole fraction of this layer results in selectivity for oxidation in comparison with the AlGaInAs of the Bragg layers. The oxidation of  $\text{Al}_{0.22}\text{In}_{0.78}\text{As}_{0.47}\text{P}_{0.53}$  layer has been performed in a normal oven with water vapor produced adjacent to the oven at 85 C. The aperture diameter is controlled through the calibration of temperature and oxidation time with aperture diameter. The produced VCSEL core diameter was maintained at 7 $\mu\text{m}$ , using a mesa of 20-21 $\mu\text{m}$ .

The two Bragg mirrors of the VCSEL structure consist of  $\text{Al}_{0.05}\text{Ga}_{0.42}\text{In}_{0.53}\text{As}/\text{InP}$  alternating layers with refractive index difference of 0.63. The energy bandgaps of  $\text{Al}_{0.05}\text{Ga}_{0.42}\text{In}_{0.53}\text{As}$  and InP have been found to be 0.8eV and 1.35eV, and their indices of refraction are 3.8 and 3.17, respectively. The top p-DBR is designed to be doped with Be at concentrations of about  $10^{19}\text{cm}^{-3}$ , and the bottom n-DBR is doped with Si up to  $5 \times 10^{18}\text{cm}^{-3}$ . The quarter wavelength thicknesses of  $\text{Al}_{0.05}\text{Ga}_{0.42}\text{In}_{0.53}\text{As}$  and InP alternating layers for both DBRs have been calculated to be 101.7nm and 121.9nm, respectively. The expected mirror reflectivities are 97% for the top DBR consisting of 16 pairs of  $\text{Al}_{0.05}\text{Ga}_{0.42}\text{In}_{0.53}\text{As}/\text{InP}$  layers, and 99.9% for the bottom DBR consisting of 22 pairs.

The p-type interconnect to the p+ DBR layer (AlGaInAs) was InSnO (ITO), which was rf sputter deposited to a thickness of 50nm. The ITO layer was deposited in a ratio of 5:1 of argon to oxygen at a total pressure of 5mTorr. A 200nm passivation of silicon dioxide was rf sputter deposited in order to dielectrically isolate the mesa structure and to provide some degree of additional sidewall protection. Sidewall coverage was achieved by rotating the wafer during sputter deposition. The contact to the n+ InP substrate was achieved through the sintered AuGeNi at 450C and 3 minutes. It is noted that the mesas were defined by reactive ion etching using a silicon nitride mesa etch mask which encapsulates the top metal contact.

The simulation of the designed VCSEL performance has been carried out by evaluation of the important laser characteristics such as threshold gain, threshold current density and external quantum efficiency. The material gain  $g_{th}$  required to reach threshold and to overcome the absorption losses in the investigated VCSEL was found to be equal to  $198\text{cm}^{-1}$  using the following equation<sup>10</sup> (1):

$$N_w \Gamma_w \xi g_{th} = \alpha + \frac{1}{2L} \ln \frac{1}{R_t R_b} \quad (1)$$

where  $N_w=8$  is the number of quantum wells in the active region,  $\Gamma_w=0.015$  is the average optical confinement coefficient per quantum well<sup>7</sup>,  $R_t=0.97$  and  $R_b=0.999$  are the reflectivities of the top and bottom Bragg mirrors, respectively,  $L=8949.9\text{nm}$  is the cavity length, and  $\xi=2$  is the energy confinement factor<sup>11</sup> or gain enhancement factor where thin active layer is at the maxima of the electric field standing wave. The optical loss<sup>12</sup>,  $\alpha=30\text{cm}^{-1}$ , includes absorption in the cladding and active layers, and scattering due to defects and inhomogeneities in the lasing medium.

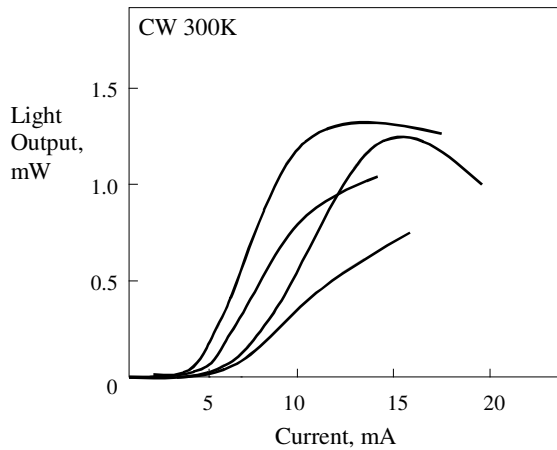
The threshold current density equal to  $J_{th} = 708\text{A}/\text{cm}^2$  with transparency current density<sup>7</sup> of  $J_{tr} = 70\text{A}/\text{cm}^2$  was calculated from the exponential dependence of  $J_{th}$ , on the device material parameters as shown in Eq.(2):

$$J_{th} = \frac{N_w J_{tr}}{\eta_i} \exp \left( \frac{\alpha + \frac{1}{2L} \ln \frac{1}{R_t R_b}}{N_w \Gamma_w \xi g_0} \right) \quad (2)$$

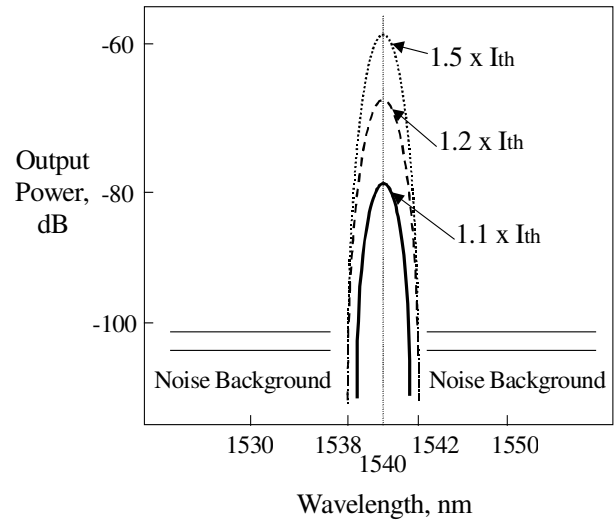
where  $\eta_i=0.9$  is the internal quantum efficiency<sup>11</sup>, and  $g_0=1575\text{cm}^{-1}$  is the material gain coefficient<sup>13</sup>. The external quantum efficiency of the structure,  $\eta_d$ , equal to 0.33, is estimated using equation (3):

$$\eta_d = \eta_i \frac{\ln \frac{1}{\sqrt{R_t R_b}}}{\alpha L + \ln \frac{1}{\sqrt{R_t R_b}}} \quad (3)$$

Assuming that VCSEL mesa structure has a diameter of  $20\mu\text{m}$ , the calculated threshold current is  $I_{th} = AJ_{th} = 2.2 \text{ mA}$ . The theoretical evaluation of the laser performance is consistent with the experimental results. The average threshold current measured for the VCSELs was  $3 \text{ mA}$  and the power output exceeded  $1\text{mW}$ . Typical light-current characteristics for four different  $20\mu\text{m}$  diameter VCSELs are presented in Figure 2 at the threshold voltage of  $2\text{V}$ . Low threshold continuous wave RT operation is achieved from all the VCSEL structures. The difference in light output power between the presented VCSELs is probably due to the variation in oxidation depth from mesa to mesa resulting in a variation of the recombination current component at the sidewall. We estimated a series resistance of a Bragg mirror to be on the order of  $500 \text{ Ohms}$  for small currents. The laser spectrum in Figure 3 from a  $7\mu\text{m}$  oxide aperture diode shows a single mode of operation at  $1.54 \mu\text{m}$ . The single fundamental mode was present at all current levels. The investigated VCSEL structure has the advantage of uniform current injection and simple processing which requires no regrowth, critical alignments, or implants.



**Figure 2.** Light-Current characteristics of the typical VCSELs.



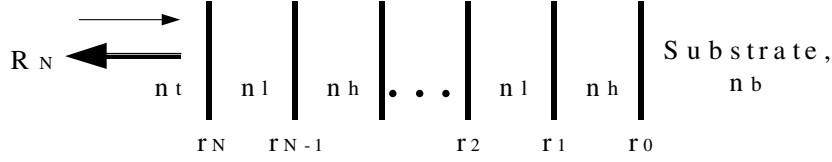
**Figure 3.** VCSEL Output Power vs. wavelength.

## 1. RESULTS AND DISCUSSIONS

Several types of composition graded interfaces were investigated as an effective method of lowering series resistance of the multilayer mirror stack. To predict reflectivity of the mirror with graded hetero-interfaces we used Airy's expressions for reflection coefficient. The reflectivity,  $R_1$ , of the two-interface stack as shown in Figure 4 is given as:

$$R_l = \left( \frac{r_l + r_0 e^{-i\phi}}{1 + r_l r_0 e^{-i\phi}} \right)^2 \quad (4)$$

where  $r_i$  are the interface field reflectivities, and  $\phi$  is the spatial phase shift.



**Figure 4.** Schematic representation of the quarter-wave Bragg mirror with N layers.

To create a highly reflective stack all interfaces in the mirror have to reflect in phase with each other, i.e. the optical thickness of each layer should be equal to the quarter wavelength of the incoming light so that  $\phi = \pi$ . Therefore, rewriting the reflectivity  $R_1$  for the two-interface stack and introducing the reflectivity  $R_2$  of the three-interface stack, we obtain:

$$R_l = \left( \frac{|r_l| + |r_0|}{1 + |r_l||r_0|} \right)^2 \text{ and } R_2 = \left( -\frac{|r_2| + R_1}{1 + |r_2|R_1} \right)^2 \text{ with } r_i = \frac{n_h - n_l}{n_h + n_l} = \frac{1 - n_l/n_h}{1 + n_l/n_h} \quad (5)$$

where  $n_h$  and  $n_l$  are high and low refractive indices of the alternating layers in the stack. The peak reflectivity of the quarter-wavelength stack with N-interfaces is then written as:

$$R_N = \left( \frac{1-b}{1+b} \right)^2 \text{ where } b = \prod_{j=0}^N \frac{n_l}{n_h} = \frac{n_t}{n_h} \left( \frac{n_l}{n_h} \right)^{N-1} \frac{n_l}{n_b} \quad (6)$$

where  $n_b$  and  $n_t$  are the refractive indices of the substrate and top layer. In our design  $n_b$  equals to  $n_l$ . By rewriting parameter  $b$ , we introduce coupling coefficient,  $\kappa$ , for the stacks with different grading types:

$$b = \frac{n_t}{n_h} \left( \frac{n_{av} - \Delta n/2}{n_{av} + \Delta n/2} \right)^{N-1} = \frac{n_t}{n_h} \left( 1 + \frac{1}{N} \left( \frac{2\Delta n}{\lambda} \right) \left( \frac{\lambda N}{4n_{av}} \right) \right)^{1-N} = \frac{n_t}{n_h} \left( 1 + \kappa \frac{\lambda}{4n_{av}} \right)^{1-N} \quad (7)$$

$$\text{where } n_{av} = \frac{n_h + n_l}{2} \text{ and } \Delta n = n_h - n_l$$


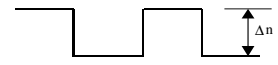

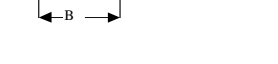
Different coupling coefficients that were used in the calculation are given in Table 1<sup>15</sup>. Therefore, the peak reflectivity of the mirror stack is given as:

$$R_N = \left( \frac{1 - \frac{n_t}{n_h} \left( 1 + \kappa \frac{\lambda}{4n_{av}} \right)^{1-N}}{1 + \frac{n_t}{n_h} \left( 1 + \kappa \frac{\lambda}{4n_{av}} \right)^{1-N}} \right)^2 \quad (8)$$

The dependence of the Bragg mirror reflectivity on the grading interface types is presented in Figure 5. We considered the bottom n-DBR mirror with 22 pairs of  $\text{Al}_{0.05}\text{Ga}_{0.42}\text{In}_{0.53}\text{As}$  ( $n_h = 3.8$ ) and  $\text{InP}$  ( $n_l = 3.17$ ) alternating layers at the incident wavelength of  $1.55\mu\text{m}$ . The  $\text{InP}$  substrate index of refraction is  $n_b = 3.17$  and top  $\text{Ga}_{0.03}\text{In}_{0.97}\text{As}_{0.07}\text{P}_{0.93}$  cladding

layer index of refraction is  $n_t = 3.2$ . The highest reflectivity is obtained through the abrupt or square composition grading at the hetero-interfaces. The sinusoidal type of grading results in reflectivity lower than for the square profile but higher than for the triangle grading profile. The linear composition grading has its upper limit as a square profile ( $A = 0$ ) and lower limit as triangle profile ( $A = B$ ). We believe that linear grading method is more effective and flexible for lowering of the series resistance in DBR stack than the other techniques since 20% linear grading at the interface results in less than 1% difference in the reflectivity of the whole stack. We compared experimentally the degradation of absorption for two linear graded samples of InGaAlAs/InP structure as shown in Figure 6. The data was taken with a 488nm Ar laser, a 0.27m spectrometer and a lock-in amplifier. The absorption as well as reflectivity spectra show spreading and degradation as the degree of grading at the interface increases.

**Table 1.** Different types of composition graded interfaces. Each coupling coefficient corresponds to a particular index profile.

Index Profile	Coupling coefficient
	$\kappa_{sin} = \frac{\pi \Delta n}{2 \lambda}$
	$\kappa_{sq} = \frac{2 \Delta n}{\lambda}$
	$\kappa_{tri} = \frac{4 \Delta n}{\pi \lambda}$
	$\kappa_{ln} = \frac{\sin x}{x} \kappa_{sq}, \quad x \equiv \frac{\pi A}{2 B}$

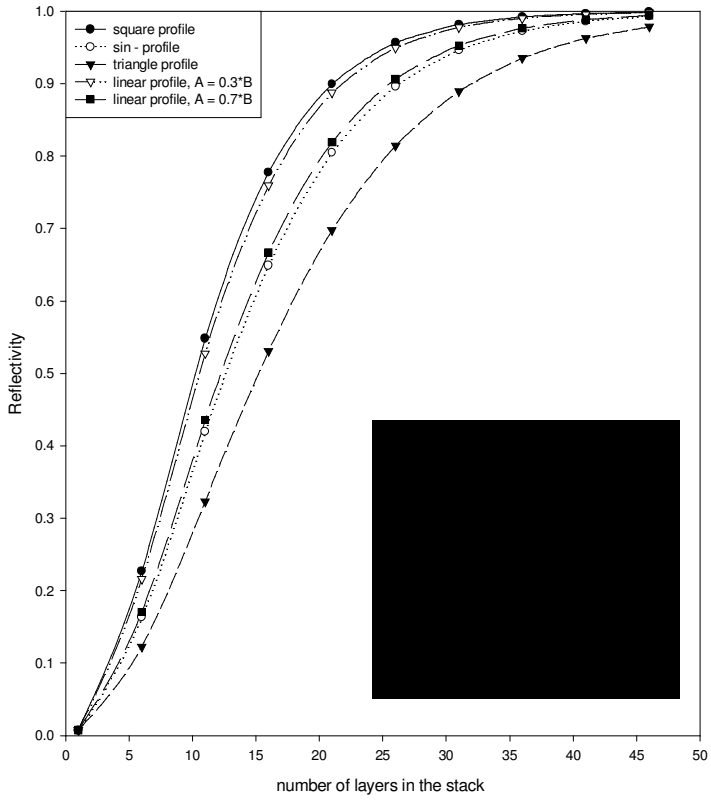


Figure 5. Reflectivity of the DBR stack as a function of different composition grading profiles

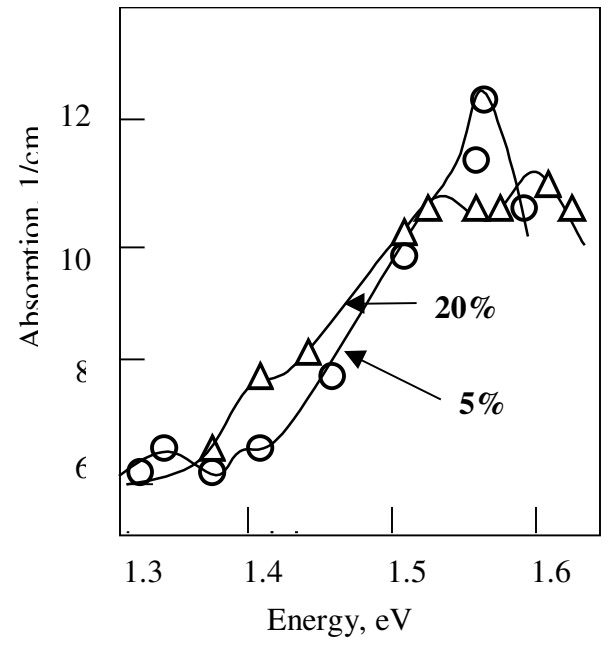
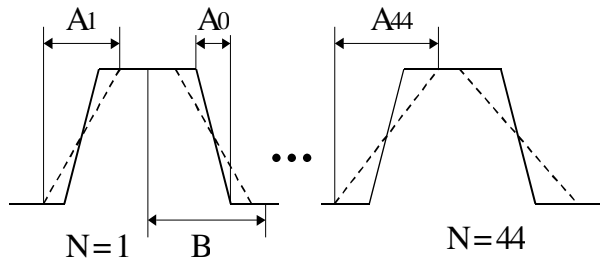
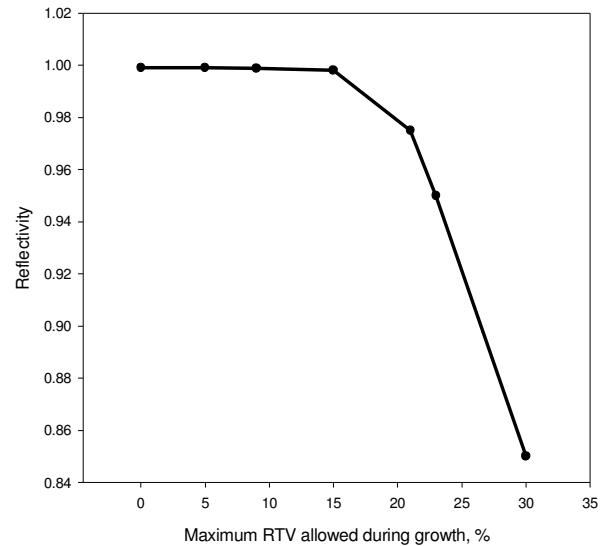


Figure 6. Absorption spectra at 30K as a function of the interface linear grading percent.

Total reflectivity of the DBR stack depends not only on the initial mirror parameters such as number of layers, index of refraction difference, and initial grading profile, but also on the growth parameters and conditions. We investigated the effect of the surface roughness and interdiffusion at the hetero-interfaces during growth on the reflectivity of the n-DBR stack and the device threshold current. A 20% constant linear grading of all layers is assumed with parameter  $A_0=0.2B=22.4\text{nm}$  as shown in Figure 7. In addition, the surface roughness is presented that increases the ideal A value. At the substrate, surface roughness equals 5% of the layer thickness, and after 44 layer are grown surface roughness equals 10% of the layer thickness. Since interdiffusion at the interface increases with time, higher diffusivity lengths would be found in the layers closer to the substrate. It was found that the change in the parameter A due to the interdiffusion is negligible. The diffusion length for the first layer is only 0.05nm at the growth temperature of 550C, growth rate of  $1\mu\text{m}$  per hour, and interdiffusion coefficient at InGaAlAs/InP interface<sup>16</sup> of  $3\times 10^{-22}\text{cm}^2/\text{s}$ . The diffusion length for the 43-rd layer interface is found to be 0.007nm. The contributions from surface roughness and interdiffusion effects result in the net increase of the parameter A from 28.9nm at layer  $N=1$  to 40.5nm at layer  $N=44$ , as shown in Figure 7. Therefore, for the assumed growth conditions, surface roughness has much stronger effect on the change in composition grading than interdiffusion of atoms at the interfaces. The reflectivity of the stack was found to be changed from 99% for ideal grading  $A_0=0.2B$ , to 92%, taking into account surface roughness and diffusivity of atoms. The VCSEL threshold current dropped from 2.3mA to 12.4mA, respectively, as estimated from Eq.(1,2).



**Figure 7.** The dynamics of the linear graded profile induced by surface roughness and interdiffusion at the interfaces as compared to the ideal constant grading  $A_0$ . The change in the parameter A at 44<sup>th</sup> layer is bigger than that at the first layer,  $A = A_0 + \Delta A$ .



**Figure 8.** Reflectivity of the mirror with 22 pairs as a function of maximum allowed RTV during growth.

The effect of random thickness variation (RTV) in the mirror layers during growth is also investigated. The thickness variations are expressed as a percentage of the ideal layer thickness. A random number generator was used to generate modified thickness depending on the allowed thickness deviations. The reflectivity of n-DBR stack was calculated as a function of maximum allowed percent change in RTV during growth as presented in Figure 8. Transfer Matrix Method was used for the reflectivity calculations<sup>15</sup>. The investigation shows that reflectivity of the stack with maximum allowed RTV higher than 15% reduces dramatically which results in a significant degradation of the mirror properties. Figure 9 presents a comparison between three reflectivity spectrums of the n-DBR stack with 22 pairs of layers. The reflectivity spectrum of the stack with RTV of 10% shows some deviations from the ideal case with RTV=0%, the peak reflectivity is still centered at  $1.55\mu\text{m}$  and equals to 99.8%. However, a much more degraded reflectivity spectrum is produced in case of RTV equal to 20% of the ideal layer thickness. The threshold current was found to be 2.3mA with RTV is no more than 10% of the initial layer thickness, however the threshold current reached 10mA for 20% RTV limit. Therefore, the random deviation in growth thickness of more than 10% will be intolerable in case where a highly reflecting mirror is desired.

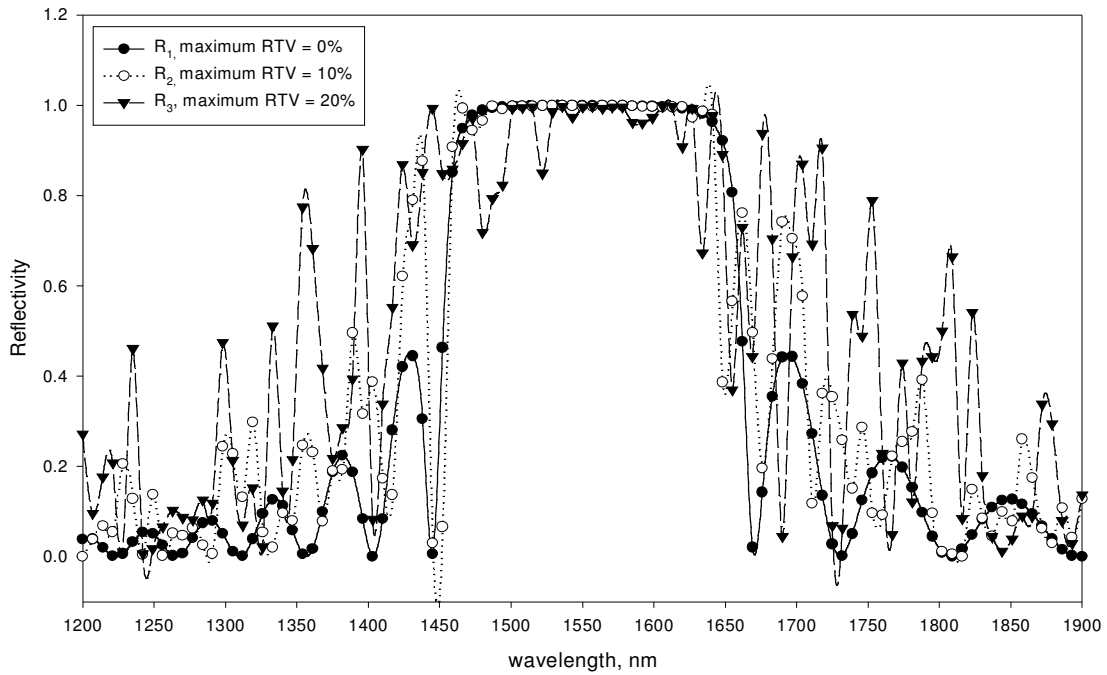


Figure 9. Reflectivity spectrum as a function of wavelength and maximum allowed RTV in the layer thickness of the 22 pair n-DBR.

Another common source of error in mirror growth can arise from a fixed bias in the grown layer thickness that may result from inaccurate calibration of the system. Reflectivity spectra were calculated for three different thickness biases. As shown in Figure 10, reflectivity spectrum  $R_2$  corresponds to 44 layer stack with each layer thicker than ideal one by 10%, and  $R_3$  spectrum has fixed thickness bias of 20%. Comparing the ideal spectrum  $R_1$  with  $R_2$  and  $R_3$  we conclude that a constant bias in the layer thickness values will result in a shifting of the reflectivity spectrum towards different lasing wavelength without decreasing its peak value.

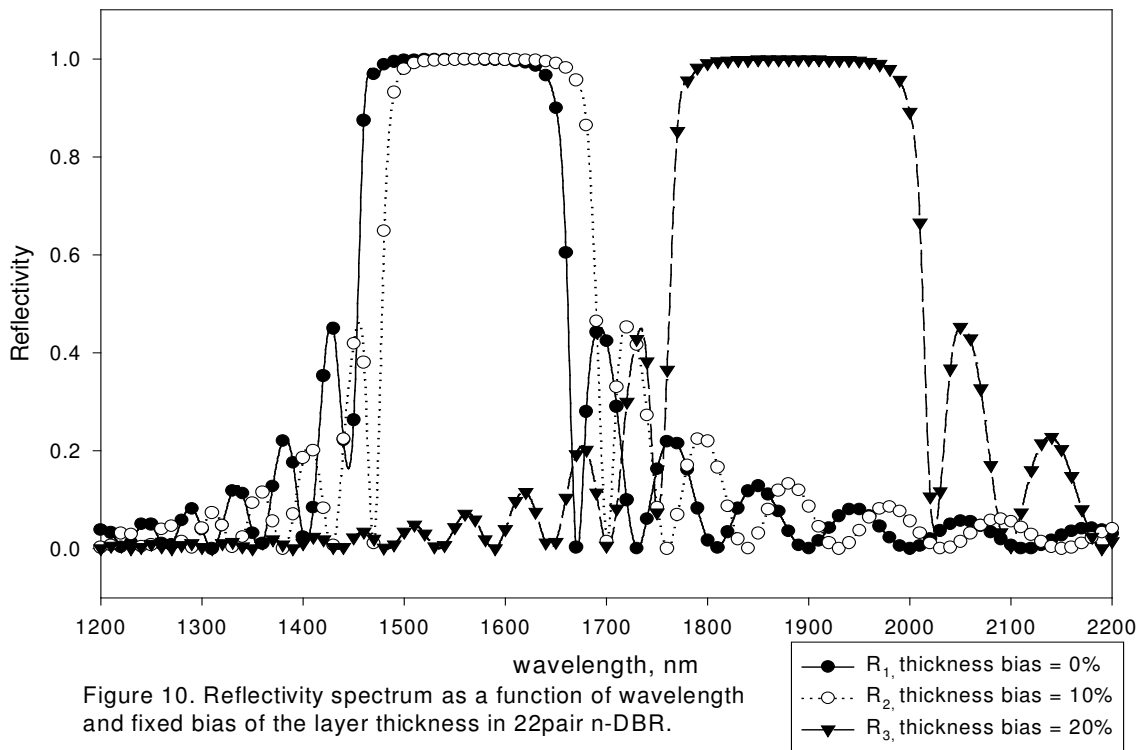


Figure 10. Reflectivity spectrum as a function of wavelength and fixed bias of the layer thickness in 22pair n-DBR.



## 2. SUMMARY

The present work demonstrates the design and performance of the epitaxial VCSEL structure based on III-V quaternary alloys for operation at 1.55 $\mu\text{m}$ . The effect of intentional and growth-related composition grading at the DBR heterointerfaces on the reflectivity of DBR and VCSEL threshold current is reported. The linear composition grading type of the hetero-interfaces is suggested to be the most suitable for the reducing of the DBR series resistance. Surface roughness is found to have a very strong effect on the reflectivity of the DBR stack as well as on the overall VCSEL performance. The random thickness variations in the mirror layers result in the distortion of the reflectivity spectrum. Finally, the fixed bias of the layer thickness introduced during growth leads to the shifting of the reflectivity spectrum. The strong dependence of the reflectivity and the threshold current on the thickness variation suggests that precise thickness control is required for DBR fabrication to match the center wavelength of the DBR to oscillation wavelength as well as for the growth of high quality VCSELs.

## ACKNOWLEDGMENTS

The investigation was funded by the Army Research Laboratory under the Microelectronics Research Cooperative Agreement, and partially by the University of Maryland Materials Research Science and Engineering Center.

## REFERENCES

1. T. Tadokoro, H. Okamoto, Y. Kohama, T. Kawakami, and T. Kurokawa, "Room temperature pulsed operation of 1.5 $\mu\text{m}$  GaInAsP/InP vertical cavity surface emitting laser", *IEEE Photon. Techn. Lett.* **4**(5), pp.409-411, 1992.
2. F. Choa, Y. Lee, T. Koch, C. Burrus, B. Tell, J. Jewell, and M. Leibenguth, "High-speed modulation of vertical-cavity surface-emitting lasers", *IEEE Photon. Techn. Lett.* **3**(8), pp.697-699, 1991.
3. J. Fastenau, and G. Robinson, "Low-resistance visible wavelength distributed Bragg reflectors using small energy band offset heterojunctions", *Appl. Phys. Lett.* **74**(25), pp.3758-3760, 1999.
4. M. Peters, B. Thibeault, D. Young, J. Scott, F. Peters, A. Gossard, and L. Coldren, "Band gap engineering digital alloy interfaces for low resistance vertical cavity surface emitting lasers", *Appl. Phys. Lett.* **63**(25), pp.3411-3413, 1993.
5. R. Moon, G. Antypas, and L. James, "Band gap and lattice constant of GaInAsP as a function of alloy composition", *J. Electr. Mater.* **3** (3), pp.635-644, 1974.
6. S. Adachi, "Band gaps and refractive indices of AlGaAsSb, GaInAsSb, and InPAsSb: key properties for a variety of the 2-4 $\mu\text{m}$  optoelectronic device applications", *J. Appl. Phys.* **61**(10), pp.4869-4876, 1987.
7. M. Rosenzweig, M. Mohrle, H. Duser, and H. Venghaus, "Threshold-current analysis of InGaAs-InGaAsP multi-quantum well separate-confinement lasers", *J. Quant Electron.* **27**(6), pp.1805-1811, 1991.
8. K. Uomi, M. Aoki, T. Tsuchiya, and A. Takai, "Dependence of high speed properties on the number of quantum wells in 1.55 $\mu\text{m}$  GaInAs-GaInAsP MWQ  $\lambda/4$ -shifted DFB lasers", *IEEE J. Quant. Electron.* **29**(2) pp.355-360, 1993.
9. B. Weigl, M. Grabherr, G. Reiner, and K. Ebeling, "High efficiency selectively oxidised MBE grown vertical-cavity surface-emitting lasers", *Electron. Lett.* **32**(6), pp.557-558, 1996.
10. G. Jones, A. Smith, E. O'Reilly, M. Silver, A. Briggs, M. Fice, A. Adams, P. Greene, K. Scarrott, and A. Vranic, "The influence of tensile strain on differential gain and Auger recombination in 1.5 $\mu\text{m}$  multiple-quantum-well lasers", *J. Quant. Electron.* **34**(5), pp.823-833, 1998.
11. G. Yang, M. MacDougal, V. Pudikov, and P. Dapkus, "Influence of Mirror Reflectivity on Laser Performance of Very-Low-Threshold Vertical-Cavity Surface-Emitting Lasers", *IEEE Photon. Techn. Lett.* **7**(11), pp.1228-1230, 1995.
12. K. Iga, F. Koyama, and S. Kinoshita, "Surface emitting semiconductor lasers", *IEEE J. Quant. Electron.* **24**(9), pp.1845-1855, 1988.
13. T. Makino, "Analytical formulas for the optical gain of quantum wells", *IEEE J. Quant. Electron.* **32**(3), pp.493-501, 1996.
14. S. Corzine, R. Yan, and L. Coldren, "A Tanh substitution technique for the analysis of abrupt and graded interface multilayer dielectric stacks", *IEEE J. Quant. Electr.* **27**(9), pp.2086-2090, 1991.
15. K. Makita, and K. Taguti, "Crystallinity and Interdiffusion in InP/InGaAs quantum wells grown by hydride VPE", *Superlatt. And Microstr.* **4**(1), pp.101-105, 1988.